Chapter 1
Carbon Dots Synthesized from Green Precursors with an Amplified Photoluminescence: Synthesis, Characterization, and Its Application

Lan Ching Sim, Jun Yan Tai, Jia Min Khor, Jing Lin Wong, Jie Yet Lee, Kah Hon Leong, Pichiah Saravanan, and Azrina Abd Aziz

Contents

L. C. Sim (✉)
Department of Environmental Engineering, Faculty of Engineering and Green Technology, Universiti Tunku Abdul Rahman, Kampar, Perak, Malaysia
e-mail: simcl@utar.edu.my

J. Y. Tai · J. M. Khor · J. L. Wong · J. Y. Lee · K. H. Leong
Department of Environmental Engineering, Faculty of Engineering and Green Technology, Universiti Tunku Abdul Rahman, Kampar, Perak, Malaysia

P. Saravanan
Department of Environmental Science and Engineering, Indian Institute of Technology (ISM), Dhanbad, Jharkhand, India

A. A. Aziz
Faculty of Engineering Technology, Universiti Malaysia Pahang, Kuantan, Pahang, Malaysia

R. Prasad (ed.), *Plant Nanobionics*, Nanotechnology in the Life Sciences,
https://doi.org/10.1007/978-3-030-16379-2_1

1.1 Carbon Dots (CDs)

Recently, carbon- or graphite-based quantum dots have gained growing attention in environmental applications, owing to its unique optoelectronic properties, broadband optical absorption, bright fluorescence emissions, favorable photoinduced electron transfer properties, and cost-effectiveness in synthesis routine (Yan et al. 2016). Accidentally discovered by Xu et al. in 2004 during purification of single-wall carbon nanotubes (SWCNTs) (Xu et al. 2004), carbon dots (CDs) have recently emerged as a new class of semiconductor due to its distinct properties, e.g., excellent photostability, excitation wavelength dependent fluorescence, low toxicity, effective infrared-responded upconverted photoluminescence (UCPL), and tunable fluorescence emission (Essner et al. 2016; Sachdeva and Gopinath 2015; Jelinek 2017). They are known as quasi-spherical shape nanoparticles with sizes below 10 nm that encompass a carbonegic core with surface functional group (Wang et al. 2017). CDs consist of graphitic carbon (sp^2 carbon) and graphene oxide sheets where the diamond-like sp^3-hybridized carbon is present, stabilizing the CDs three-dimensional network (Demchenko and Dekaliuk 2013). The carboxyl groups on the surface of CDs provide great water solubility and enable the advance functionalization with chemically reactive group and surface passivation with organic, inorganic, polymeric, or biological materials to CDs that could enhance fluorescence properties of CDs (Lim et al. 2015; Baker and Baker 2010).

CDs possess excellent fluorescence characteristic and high photostability against photobleaching and blinking which potentially become an alternative to heavy metal-based semiconductor quantum dots (SQDs) currently in use (Wang et al. 2011). Although SQDs like CdSe, CdS, and PbSe were widely used due to their strong photostability, fluorescence, and tunable emission, their high toxicity has raise safety concern of environment and human's health, restricting both biological and environmental application. The differences between CDs and SQDs are that luminescence of CDs emits from the surface, whereas in the latter case, luminescence originates from the core of the nanocrystals (Štěpánková et al. 2015). So by attaching the carboxyl, hydroxyl, and amino groups on the surface of CDs, the optical property and biocompatibility as well as the selectivity and sensitivity could be enhanced. CDs are able to emit PL under near-infrared (NIR) light excitation that given a potential for light energy conversion, photovoltaic devices, and related applications (Wang et al. 2009). The PL intensity of CDs tends to reduce when the pH turns alkaline, making it suitable for cellular imaging (Pandey et al. 2013). CDs are also used as bio-sensing for visual monitoring of glucose, potassium, nucleic acid, copper, and pH (Namdari et al. 2017).

The photoluminescence (PL) of CDs is dependent on quantum effect of nanoparticles with various sizes, emissive traps on the surface of CDs, excitation wavelength (λ_{ex}), or other unknown factors (Wang and Hu 2014; Baker and Baker 2010). The PL of CDs can be efficiently quenched by electron acceptor or donor molecules in solution, indicating that photoexcited CDs exhibit excellent electronic properties as electron donor and acceptor (Zhang and Yu 2015). Besides that, it also can act as an electron mediator, photosensitizer, and spectral converter due to its UCPL property (Wang et al. 2009a). Thus, it is not surprising that the applications of CDs have been extended to photocatalysis of water splitting and removal of organic pollutants in recent years. Nevertheless, the mass fabrication and selection of an appropriate precursor that is low cost, sustainable, high carbon yield, and easily available for long period of time (Zhu et al. 2013) are the main challenges facing by CDs.

1.2 Carbon Dots Synthesized from Green Precursors

Recently, CDs derived from green precursors (green CDs) have gained attention from numerous researchers because of its excellent properties and also environmentally friendly synthesis routine (Yan et al. 2016). The "green precursors" are defined as derivatives of renewable natural products or processes or naturally occurring (Sharma et al. 2017). Green CDs show much more promise in greener and sustainable future development as most of the natural resources can be obtained economically and also synthesized using versatile method (Shen and Liu 2016). In past researches, various chemical precursors such as glucose (Ma et al. 2012), citric acid (Ju et al. 2014; Schneider et al. 2017), ethylene glycol (Wang et al. 2017b), and EDTA (Liu et al. 2017) were widely reported. Since CDs are mainly applied for biomedicine application such as drug delivery, biosensing, bioimaging, and gene transfer, the switch from chemical precursors to "green precursors" is more appropriate. The green precursors can be obtained from natural resources such as sugarcane juice (D'souza et al. 2016; Sim et al. 2018), pomelo peels (Lu et al. 2012), willow bark (Qin et al. 2012), and bagasse (Du et al. 2014) (Fig. 1.1). Hydrothermal carbonization method is widely used to prepare CDs from green materials due to its low cost, nontoxic nature, and environmentally friendly process. The quantum yield (QY) of CDs is based on the type of green precursors and preparation method used, as shown in Table 1.1.

Nitrogen doping in CDs has been reported recently to increase the QY and to improve the intrinsic low emission efficiency. Liu et al. (2012) successfully increased the QY of grass-derived CDs from 2.5% to 6.2% after doping with nitrogen. One-pot hydrothermal carbonization method was used by Liao et al. (2016) to produce water-soluble nitrogen-doped CDs (N-CDs) from the mixture of natural peach gum polysaccharide (PGP) and ethylenediamine. The QY of N-CDs was enhanced from 5.31% to 28.46% after surface passivation of CDs with nitrogen (Liao et al. 2016). Ethylenediamine was also used as a nitrogen source to produce N-CDs from onion wastes (Bandi et al. 2016) with QY of 28%. Liu et al. (2017a)

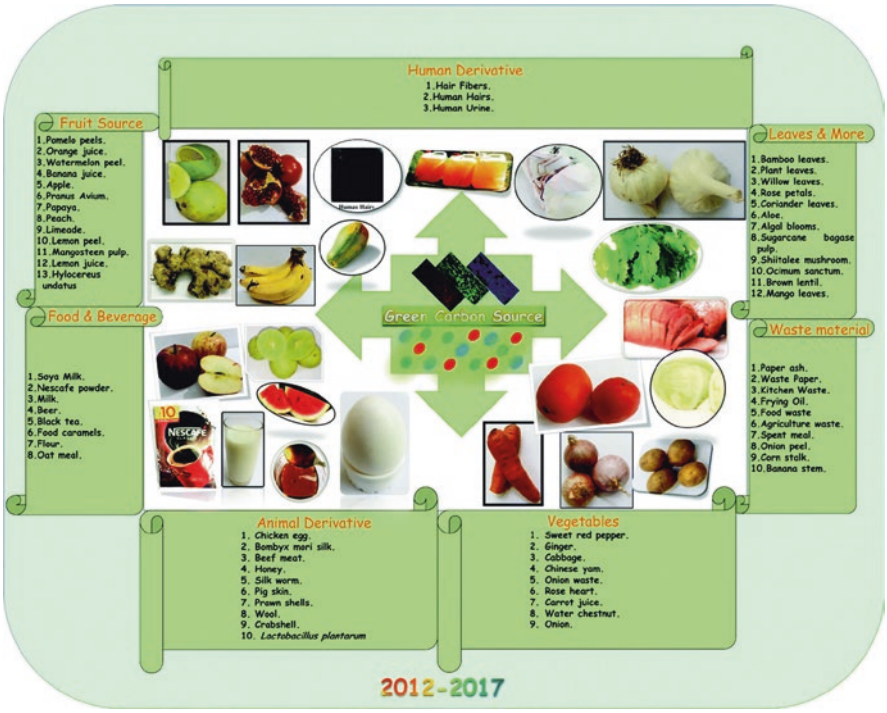

Fig. 1.1 Green precursors used to produce CDs. (From Sharma et al. 2017)

used ammonia as nitrogen source to dope CDs derived from rose-heart radish and achieved a QY of 13.6%. Ding et al. (2017) used pulp-free lemon juice as intrinsic nitrogen source to prepare CDs with high QY (28%) and intense red luminescence. High-protein sources such as milk (Wang and Zhou 2014), chicken egg (Wang et al. 2012), oatmeal (Yu et al. 2015), hair (Guo et al. 2016), etc. were used as intrinsic nitrogen sources for the self-passivation of CDs. Among these intrinsic sources, oatmeal successfully produced N-CDs with the highest QY (37.4%) due to the highest N/C ratio prepared at 200 °C (Yu et al. 2015). Besides N-doping of CDs, other researchers also produced the nitrogen- and sulfur-co-doped CDs (N-S-CDs). Sun et al. (2013) developed a large-scale synthesis of N-S-CDs by using sulfuric acid carbonization and etching of hair fiber. They claimed that higher reaction temperature at 140 °C was favorable to form N-S-CDs with smaller size, higher S content, and longer wavelength of photoluminescence emissions. A greener method was reported by Zhao et al. (2015), where N-S-CDs were prepared using garlic as intrinsic source for N and S doping without using harmful chemicals like sulfuric acid as sulfur source. The obtained CDs possess good water dispersibility and quantum yield of 17.5%.

Table 1.1 Synthetic method and quantum yield of different precursors

Precursor	Synthetic method	Quantum yield (%)	Particle size (nm)	References
Orange juice	Hydrothermal treatment at 120 °C	26	1.5–4.5	Sahu et al. (2012)
Strawberry juice	Hydrothermal treatment at 120 °C	6.3	5.2	Huang et al. (2013)
Sugarcane juice	Hydrothermal treatment at 120 °C	5.76	3	Mehta et al. (2014)
[a]Grass	Hydrothermal treatment at 150–200 °C	2.5–6.2	3–5	Liu et al. (2012)
Orange peels	Hydrothermal 180 °C for 12 h.	36	2–7	Prasannan and Imae (2013)
Waste paper	Hydrothermal with urea, 150 °C for 50 min	–	–	Fadllan et al. (2017)
Papaya juice	Hydrothermal 150 °C for 12 h.	7	3	Kasibabu et al. (2015)
Tulsi leaves	Hydrothermal 180 °C for 4 h	9.3	4–7	Kumar et al. (2017)
[a]Milk	Hydrothermal treatment at 180 °C	12	2–4	Wang and Zhou (2014)
Hair	Carbonization at 200 °C	10.75	2–8	Guo et al. (2016)
Coriander leaves	Hydrothermal treatment at 240 °C	6.48	4.1	Sachdeva and Gopinath (2015)
Sweet potatoes	Hydrothermal treatment at 180 °C	2.8	1–3	Lu et al. (2013)
Pomelo peels	Hydrothermal treatment at 200 °C	6.9	2–4	Lu et al. (2012)
Cabbage	Hydrothermal treatment at 140 °C	16.5	2–6	Alam et al. (2015)
Willow bark	Hydrothermal treatment at 200 °C	6	5–25	Qin et al. (2012)
[a]Oatmeal	Hydrothermal treatment at 200 °C	37.4	20–40	Yu et al. (2015)
Bagasse	Hydrothermal treatment at 180 °C	9.3	12.3	Du et al. (2014)
[a]Soy milk	Hydrothermal treatment at 180 °C	2.6	–	Zhu et al. (2012)
Banana juice	Heating in oven at 150 °C for 4 h	8.95	3	De and Karak (2013)
Apple juice	Hydrothermal treatment at 150 °C	4.27	4.5	Mehta et al. (2015)
[a]Peach gum	One-pot hydrothermal carbonization of the mixture of natural peach gum polysaccharide (PGP) and ethylenediamine	28.46	2–5	Liao et al. (2016)

(continued)

Table 1.1 (continued)

Precursor	Synthetic method	Quantum yield (%)	Particle size (nm)	References
[a]Lemon juice	Hydrothermal treatment at 190 °C for 10 h	28	4.5	Ding et al. (2017)
[a]Chicken egg	Direct plasma treatment at radio-frequency power of 120 W (voltage = 50 V, current = 2.4 A)	8	2.04–3.39	Wang et al. (2012)
Urine	Carbonization at 200 °C	5.3	10–55	Essner et al. (2016)
[a]Onion	Hydrothermal treatment at 120 °C	28	7–25	Bandi et al. (2016)
[a]Rose-heart radish	Hydrothermal treatment at 180 °C for 3 h	13.6	1.2–6	Liu et al. (2017a)
[b]Hair fiber	Sulfuric acid carbonization and etching of hair fiber	11.1	3.1–7.5	Sun et al. (2013)
[b]Garlic	Hydrothermal treatment at 200 °C for 3 h	17.5	11	Zhao et al. (2015)

[a]CDs doped with nitrogen (N-CDs)
[b]CDs doped with sulfur and nitrogen (N-S-CDs)

1.3 Synthesis

Numerous synthesis approaches of CDs reported can be categorized into two major routes: top-down and bottom-up approaches. CDs can be produced and modified via physical, chemical, or electrochemical techniques during preparation or posttreatment period (Namdari et al. 2017). The unique characteristics of each CDs synthesis method were summarized in Table 1.2. During CDs synthesis, three main issues such as carbonaceous aggregation, size control and uniformity, and surface properties are needed to be addressed to create CDs with optimum properties for various applications (Wang and Hu 2014).

1.4 Top-Down Approaches

The top-down route generally involves the breaking down process of relatively large carbon structures such as activated carbon, carbon nanotubes, carbon soot, graphite, graphite oxide, and nanodiamonds via arc discharge, chemical oxidation, and electrochemical and laser ablation (Xu et al. 2014; Liu et al. 2016). The top-down approaches are typically conducted as their simple operation, and abundant raw materials allowed mass production of CDs. However, these approaches require specific treatments and would produce low yield from graphite source as most graphites have relatively large graphitic structures which are hard to be broken down to

Table 1.2 The unique characteristics of each CDs synthesis method

Approaches	Synthesis techniques	Advantages	Disadvantages	References
Top-down	Arc discharge	High production of low-defect products Environmentally benign	Low quantum yield	Liang et al. (2017), Zuo et al. (2015)
	Electrochemical	Less synthesis reaction time Does not need costly reagents, further surface modification, high temperature, and strong acid	Low quantum yield	Hou et al. (2015)
	Laser ablation	Cheap Convenient Trouble-free	Lower quantum yield Poor control over sizes	Shahidi et al. (2018), Namdari et al. (2017)
Bottom-up	Combustion	Does not use external heating sources Short reaction duration Rapid product cooling process	Requires appropriate raw material for morphology control	Baker and Baker (2010), Hossain and Islam (2013)
	Hydrothermal/ solvothermal	Environmentally friendly Low cost Nontoxic	Required high temperature	Wang and Hu (2014), Hu et al. (2010)
	Microwave irradiation	Cost-effective Energy-conservative Time-saving	Low production	Guo et al. (2017), Wang et al. (2017a)

less than 10 nm in diameter. Dong et al. (2010) found that this drawback can be slightly reduced by altering the carbon source with amorphous carbon form that contained abundant tiny crystalline graphite fragments via a suitable synthesis method. Hence, the discussion of top-down approaches is done to allow better visualization on top-down approaches.

1.4.1 Arc Discharge

Arc discharge approach is a popular method to synthesize carbon nanomaterials due to its high production of low-defect products with environmentally benign properties. The morphologies and productivity of CDs can be controlled with arc satiability and precursor temperature history as they determine the interaction at the anode boundary (Liang et al. 2017). Arora and Sharma (2014) elaborated that the arc discharge process involved the electrical breakdown of a gas to produce plasma by using electric current in alternating or direct current. The generated plasma

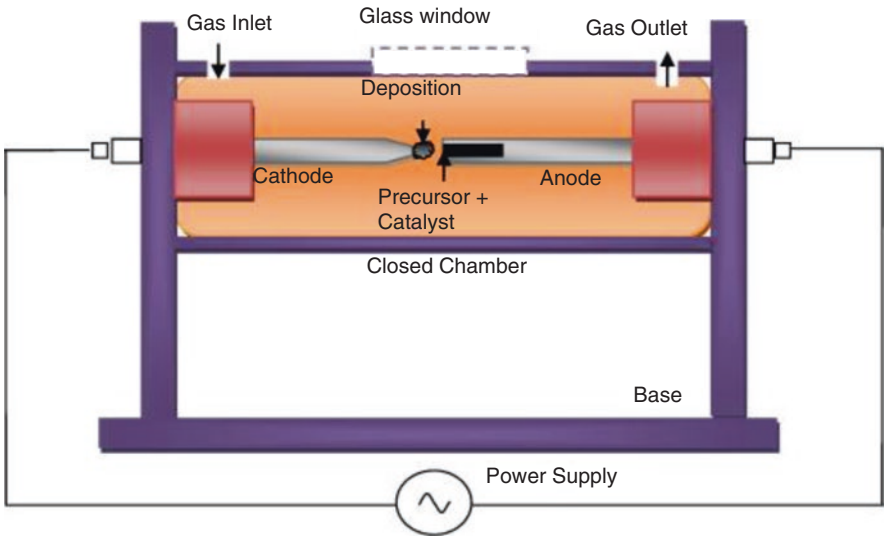

Fig. 1.2 Schematic drawing of an arc discharge setup. (From Arora and Sharma 2014)

(4000–6000 K temperature) with high heat flux or thermal energy would then sublime the bulk carbon precursor to create carbon vapors. Next, the carbon vapors would undergo phase change and transform into liquid at cooler temperature. Figure 1.2 shows the schematic drawing of an arc discharge setup. Xu et al. (2014) discovered the production of stable black and crude suspension with arc-discharge soot oxidation with nitric acid precursor and sediment extraction with sodium hydroxide aqueous solution. The black suspension separated an average of 18 nm diameter fluorescent CDs after gel electrophoresis purification method. Moreover, Bottini et al. (2006) showed that the blue to yellowish-green fluorescent range CDs were produced via arc discharge from carbon nanotubes. The discovery of argon gas breakdown in a fluid form for CDs production was pioneered by Sun et al. (2016) and allowed the elimination of agglomerated CDs by frequency adjustment. Despite that, CDs yield via arc discharge approach is still low (Zuo et al. 2015).

1.4.2 Electrochemical Carbonization

Electrochemical carbonization method is another widely employed nonselective method in top-bottom approach (Zhao et al. 2008; Ming et al. 2012). Bulk carbons such as carbon nanotubes, carbon fiber electrodes, and graphite are used in the production of carbon quantum dots. Deng et al. (2014) employed a conventional three-electrode system composed of two Pt sheets with a dimension of 4×4 cm^2 as working and counter electrode and reference electrode. The reference electrode is a calomel electrode that is mounted on freely adjustable Luggin capillary. The

applied voltage in the setup can affect size, carbon content, and UV-vis absorption and brightness of CDs similar with Bao et al.'s (2011) study. Another study done by Li et al. (2010) showed that the electrochemical carbonization synthesis of CDs was assisted by alkali. An alkaline environment played a major factor as it aids in judicious cutting of carbon honeycomb layer into ultrasmall carbon particles due to the presence of hydroxyl (OH^-) group from alkali suspension. Zhou et al. (2007) reported that the structure evolution of bulk carbon changed upon the number of cycles of electrochemical treatment. Multiwalled carbon nanotubes at 100th electrochemical treatment cycles had entangled with curled and swelling features, while 1000th electrochemical treatment cycles had caused serious deformation and tube wall openings. Therefore, the number of electrochemical treatment cycles influenced the active area and surface reaction of CDs. In comparison with other methods, this method reduces synthesis reaction time and does not need costly reagents, further surface modification, high temperature, and strong acid (Hou et al. 2015). However, the quantum yield of CDs is low with electrochemical carbonization (Zuo et al. 2015).

1.4.3 Laser Ablation

According to Shahidi et al. (2018), the laser ablation method is a convenient, cheap, and trouble-free method. This method utilizes pulsed laser with high pulse energy on target surface immersed in a liquid medium for vaporization and flume formation which contains high kinetic energy cluster, as well as atomic and ionic particles (Gondal et al. 2013). The flume would react with the liquid medium to produce CDs. However, the laser ablation in liquid medium required an additional process for common materials and did not utilize the merits of high temperature synthesis (Kazemizadeh et al. 2017). Therefore, the generation of CDs using laser ablation method was done in vacuum method to prevent the problems present in liquid medium. Gonçalves et al. (2010) stated that the laser ablation method was optimized with variation of distance between focusing lens and carbon target. The increased distance between focusing lens and carbon target increased the area of irradiated carbon target and influence which ultimately result to wider size dispersion. Sun et al. (2006) first reported that the produced CDs from laser ablation method in water with argon carrier gas showed bright luminescence upon attaching simple organic species. Simple organic compounds like diamine-terminated oligomeric polyethylene glycol (PEG_{1500N}) were used before acid treated at 120 °C for 72 h. The attachment process allowed surface passivation to occur which resulted to emissive surface energy traps upon stabilization. Kazemizadeh et al. (2017) elaborated that the middle energy levels of CDs caused thermal quenching and prevented elimination of photoluminescence radiation after surface passivation. Quantum confinement of these emissive surface energy traps also played a part as the large surface-to-volume ratio was needed for brighter luminescence. Despite their attractive merits, the laser ablation method was reported to have a lower quantum yield and poor control over sizes (Namdari et al. 2017).

1.5 Bottom-Up Approaches

Alternatively, the bottom-up approaches form selected molecular precursor to "quantum-sized" particles via combustion, hydrothermal/solvothermal, and microwave irradiation methods (Xu et al. 2013). The bottom-up approaches offered great advantages as morphology and size distribution of the product can be precisely controlled for surface passivation. The selection of precursors and synthesis methods in bottom-up approaches is needed to be addressed and discussed.

1.5.1 Combustion

Nersisyan et al. (2017) defined that the combustion technique is a complex process which involves self-sustaining chemical activities with rapid release of heat in the high-temperature reaction front form. The primary factors of the combustion process application in synthesis method are heat, light, and engines. In comparison with other techniques with high temperature, combustion technique does not use external heating sources and has short reaction duration with rapid product cooling process which allowed the production of non-equilibrium products that have unique biological, electrochemical, mechanical, and physical properties. The combustion method used soot-derived sources from candles or natural gas to synthesize CDs (Baker and Baker 2010). Soot carbon was referred to as the carbonaceous aerosol dark component which consisted of pure elemental carbon with highly polymerized organic material by Cachier et al. (1989). Hossain and Islam (2013) stated that the incomplete combustion process created nonuniform size and shape CDs. Incomplete combustion typically occurs when oxygen was insufficient for complete reaction with fuel to produce water (H_2O) and carbon dioxide (CO_2). Incomplete combustion was utilized to produce carbon soot. An example of incomplete combustion of dodecane was shown in the equation below. In reality, actual combustion process produced a wide range of major and minor products such as carbon monoxide (CO) and pure carbon (C).

$$C_{12}H_{26} + O_2 \rightarrow C + CO_2 + CO + H_2O \tag{1.1}$$

This simple and effective synthesis via combustion method was reported by Tian et al. (2009). Combustion soot of natural gas produced 5 nm diameter CDs that exhibited indirect bandgap semiconductor material behavior and electrochemical activities. Another study conducted by Rahy et al. (2012) synthesized CDs by combusting an aromatic compound in a controlled environment of a Pyrex® glass container. The aromatic compounds used are benzene, toluene, and xylene. The morphology of CDs can be controlled by usage of raw materials. Kshirsagar et al. (2017) compared different organic precursor such as almond flames, burnt almond char, clarified butter, and mustard oil for the CDs synthesis. Their study discovered

that the saturated fatty acids present in fats or oils contained high percentage of carbon for CDs synthesis. These findings would allow the utilization of food products into CDs synthesis via combustion technique.

1.5.2 Hydrothermal/Solvothermal

Hydrothermal/solvothermal synthesis method is the most widely used bottom-up method as it allowed formation of high pressure and temperature in an autoclave condition to obtain good crystal morphology of CDs (Xu et al. 2013). Hydrothermal method utilized water solvent, whereas solvothermal method used organic solvents such as benzene, dimethylformamide (DMF), or dimethyl sulfoxide (DMSO). These synthesis methods were also reported by Wang and Hu (2014) to be low cost, environmentally friendly, and nontoxic as their precursor used were of chemical or biological origins. Chemical materials such as citric acid and Tris were used in production of CDs as they were relatively cheap and environmentally friendly (Zhou et al. 2015). The citric acid- and Tris-derived CDs exhibited strong fluorescence upon contact with Fe^{3+} ions and hypotoxicity toward living cells. Other chemicals such as ethanol in hydrogen peroxide solution were able to synthesize CDs that were temperature sensitive and able to detect hypochlorite ions at high quantum yield of 38.7% without surface passivation or even heteroatom doping as described in Hu et al.'s (2016) study. The ethanol solution was used as the carbon source as it is the most common and cheap reagent in the laboratory. Similarly, nontoxic and nonimmunogenic polyethylene glycol can act as passivating solvent to produce bright, photostable, and tunable photoluminescence-emitted CDs (Fan et al. 2014). According to Sharma et al. (2017), biological materials used as green precursors for hydrothermal/solvothermal synthesis are fruits, fruit juices, fruit peels, vegetable, spices, plant leaves, beverages, animal, animal and human derivatives, and waste materials. A study by Sim et al. (2018) had reported that the CDs produced using sugarcane juices enhanced the solar photocatalytic performance of g-C_3N_4 upon coupling. Besides that, vegetables such as broccoli were also used to produce CDs that detected Ag^+ ions, as per a study by Arumugam and Kim (2018). *Bombyx mori* silk that was made up of sericin and fibroin was able to produce CDs at hydrothermal condition for cell imaging application as shown in Fig. 1.3 (Wu et al. 2013). CDs can also be synthesized using waste materials like cigarette filters to detect Sudan I dye with a high selectivity and sensitivity (Anmei et al. 2018). Despite hydrothermal/solvothermal advantages, Hu et al. (2010) reported that the hydrothermal/solvothermal method required high temperature in the synthesis method which would create impracticality in large-scale production. The low-temperature hydrothermal/solvothermal method, however, required additional metal ions or templates to produce different morphologies of carbon materials for optimization of their applications.

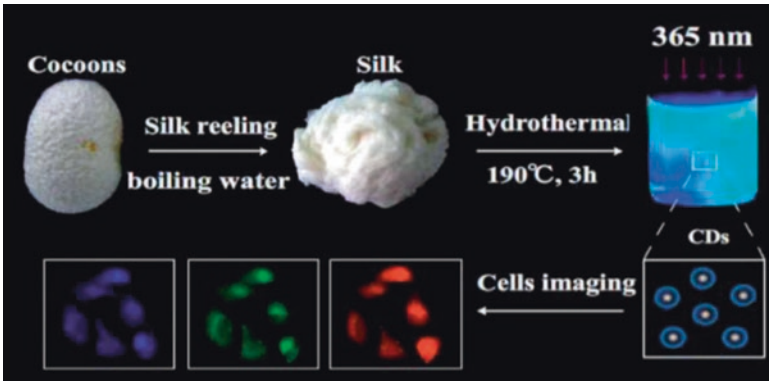

Fig. 1.3 Illustration of CDs formation for *Bombyx mori* silk. (From Wu et al. 2013)

1.5.3 Microwave Irradiation

Guo et al. (2017) stated that microwave irradiation method is an efficient synthesis method as it is time-saving, cost-effective, and energy-conservative. Microwave irradiation is located between infrared irradiation (0.001 m) and radio waves (1 m) in the electromagnetic spectrum. Microwave irradiation had a strong penetrating ability in various mediums and caused charged particle interaction (Zhang et al. 2007). The charged particle interaction changed thermodynamics function by reducing activation energy of materials and weakening the chemical bond intensities. Materials that produce heat after interaction with microwave irradiation are known as microwave absorbers. Carbon was reported to be a good microwave absorber as it generates heat upon contact with microwave irradiation, as per a research by Menéndez et al. (2010). This synthesis method was described to have a faster reaction time as compared with conventional hydrothermal/solvothermal methods (Pham-Truong et al. 2018). L-lysine-derived CDs produced in Choi et al.'s (2017) study had strong blue photoluminescence after 5 min of microwave irradiation. The produced CDs from L-lysine can be used for biological application as it had a 97% cell viability assay with KB and MDCK cells and can be exploited in cellular imaging with successful uptake through endocytosis. In addition, Wang et al. (2011) reported that the CDs produced from graphite oxide had a higher absorption and lifetime of 3.72 ns through microwave heating route. The microwave irradiation allowed materials to grow uniformly as it was able to produce force upon charge particle to move or polarize. Subsequently, the molecular movement would cause friction and collisions and, thus, generate rapid heating which eliminates temperature gradient effect. In another study done by Yang et al. (2015a), CDs produced from folic acid and urea via microwave route had good biocompatibility and cytotoxicity as they distinguished GES-1 normal cell and HeLa cancer cell. However, the present CDs production from microwave irradiation was low as it was less than 40%, and it would significantly hinder the practical application of CDs (Wang et al. 2017a).

1.6 Structural Properties

The surface properties of green precursor-derived CDs are investigated using the X-ray photoelectron spectroscopy (XPS) and Fourier-transform infrared spectroscopy (FTIR). The internal structural properties are analyzed using high-resolution transmission electron microscopy (HRTEM), Raman spectroscopy, and X-ray powder diffraction (XRD).

1.6.1 Surface Properties (XPS and FTIR)

Both XPS and FTIR results can be used to confirm the functional groups in the CDs. Figure 1.4a, b shows the CDs prepared from orange peels consist of various oxygen-containing functional groups such as C=C/C–C, C–OH/C–O–C, C=O, O–C=O, C–O, C=O, and C–OH/C–O–C. The XPS results are consistent with the FTIR spectra (Fig. 1.4c) which detected the C=C stretching of polycyclic aromatic hydrocarbon and carbonyl groups (C=O). Besides, the signals arising from the furan rings of 5-hydroxymethylfurfural and nonaromatic compounds were also detected by nuclear magnetic resonance (NMR) (Prasannan and Imae 2013). For sulfur- and nitrogen-doped CDs (S–N–CDs) derived from hair fiber, Sun et al. (2013) reported the additional existence of $–SO_3^–$, C–N, C–S, N–H, and S–H bonds in FTIR spectra which is in consistence with the XPS spectrum. The presence of –C–S- covalent bond of the thiophene-S is confirmed by the peaks at 163.5 and 164.6 eV, while the pyridinic N and pyrrolic N were observed at 398.5 and 399.7 eV. The N-CDs derived from onion are highly soluble in water and able to serve as linkers for the attachment of biomolecules owing to the presence of different functional groups such as –OH, –COOH, and –NH in N-CDs. The XPS N 1 s spectrum indicated the presence of C–N–C (398.5 eV) and N–H (400.2 eV) bonds in N-CDs which was consistent with –N–H stretching vibrations (3200–3400 cm^{-1}) and C–N stretching vibrations (1340 cm^{-1}) in FTIR spectrum (Bandi et al. 2016).

1.6.2 Internal Structural Properties (HRTEM, Raman, and XRD)

As shown in Table 1.1, the particle size of CDs varies with the type of precursors used to produce the CDs, ranging from 1 to 40 nm. Yu et al. (2015) synthesized oatmeal-derived CDs with larger particle size between 20 and 40 nm with relatively good quantum efficiency of 37.4% (Fig. 1.5a, b). Most of the reported CDs exhibit a broad diffraction peak at 25° with d-spacing ranging from 0.32 to 0.34 nm which is attributed to highly disordered carbon atoms (Zhu et al. 2013; Ding et al. 2017). The shift of diffraction peak to 22.6° and the increase of d value to 0.39 nm

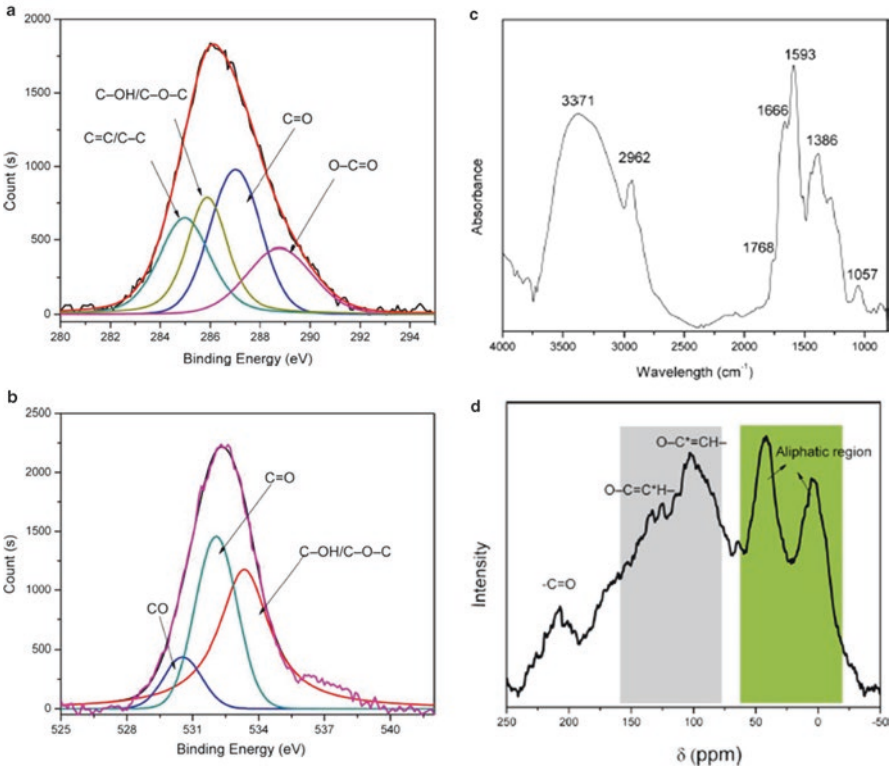

Fig. 1.4 XPS scans (**a**) C1s, (**b**) O1s regions of CDs, (**c**) FTIR spectra of CDs, and (**d**) ^{13}C solid-state NMR spectrum of CDs. (From Prasannan and Imae 2013)

(Fig. 1.5c) suggested the amorphous nature of CDs and the introduction of oxygen functional groups during the synthesis (Yu et al. 2015). Similar results were also reported by other researchers (Alam et al. 2015). The absence of lattices in CDs due to the amorphous nature was also reported by other researchers (Liao et al. 2016; Essner et al. 2016). Nevertheless, lattice spacing of 0.226 nm was observed in N-CDs derived from rose-heart radish, indicating the graphitic nature of N-CDs (Liu et al. 2017a). Alam et al. (2015) found that the lattice spacing of cabbage-derived CDs is 0.21 nm, which corresponds to sp^2 (1120) graphitic crystal phase of graphene. CDs possess several defects which can be observed in Raman spectrum. Two obvious peaks at D band (~1360 cm^{-1}) and G band (~1580 cm^{-1}) (Fig. 1.5d) are attributed to the partially disordered graphite-like structure of sp^3 and sp^2 hybrid carbons, respectively (Li et al. 2013; Yu et al. 2015).

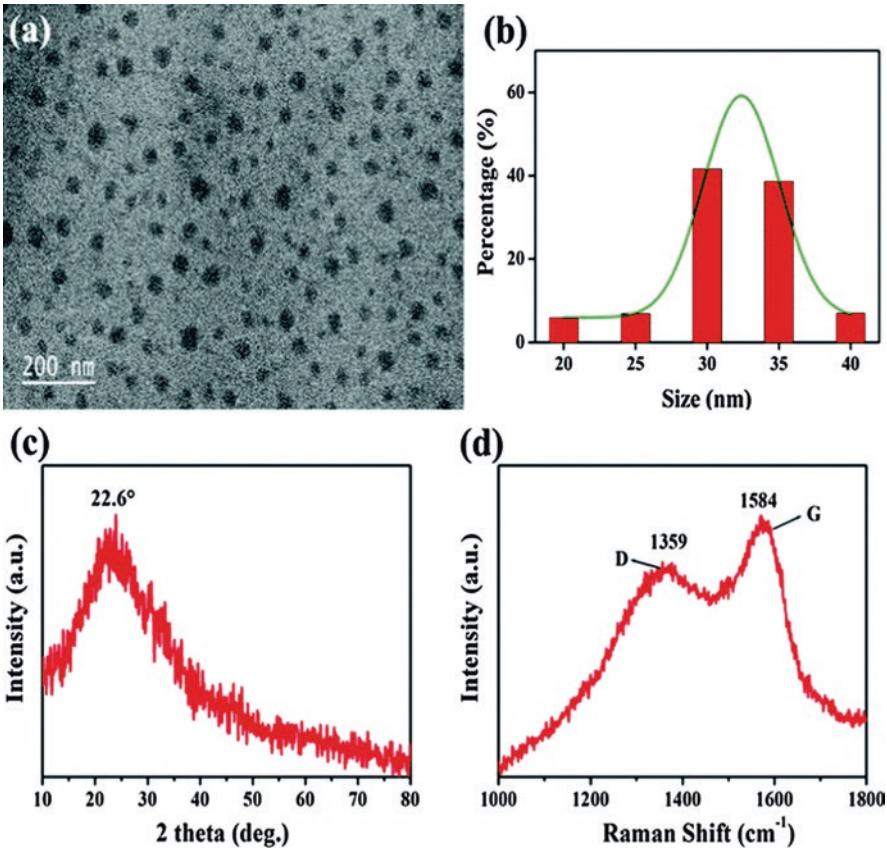

Fig. 1.5 TEM image (**a**), size distribution histogram (**b**), XRD pattern (**c**), and Raman spectrum (**d**) of the CNPs. (From Yu et al. 2015)

1.7 Other Properties

Other properties of CDs such as optical absorption, photoluminescence, upconverted photoluminescence (UCPL) properties, separation of charge carriers, and quantum yield will be discussed in following sections.

1.7.1 Optical Absorption

For coriander leaf-derived CDs solution, Sachdev and Gopinath (2015) observed two absorption peaks at 273 nm and 320 nm which were ascribed to π–π* transition of C=C bonds and n–π* transition of C=O bonds in Fig. 1.6b. Similar observation was reported by earlier researchers (Sachdev et al. 2014; Sachdev et al. 2013; Park

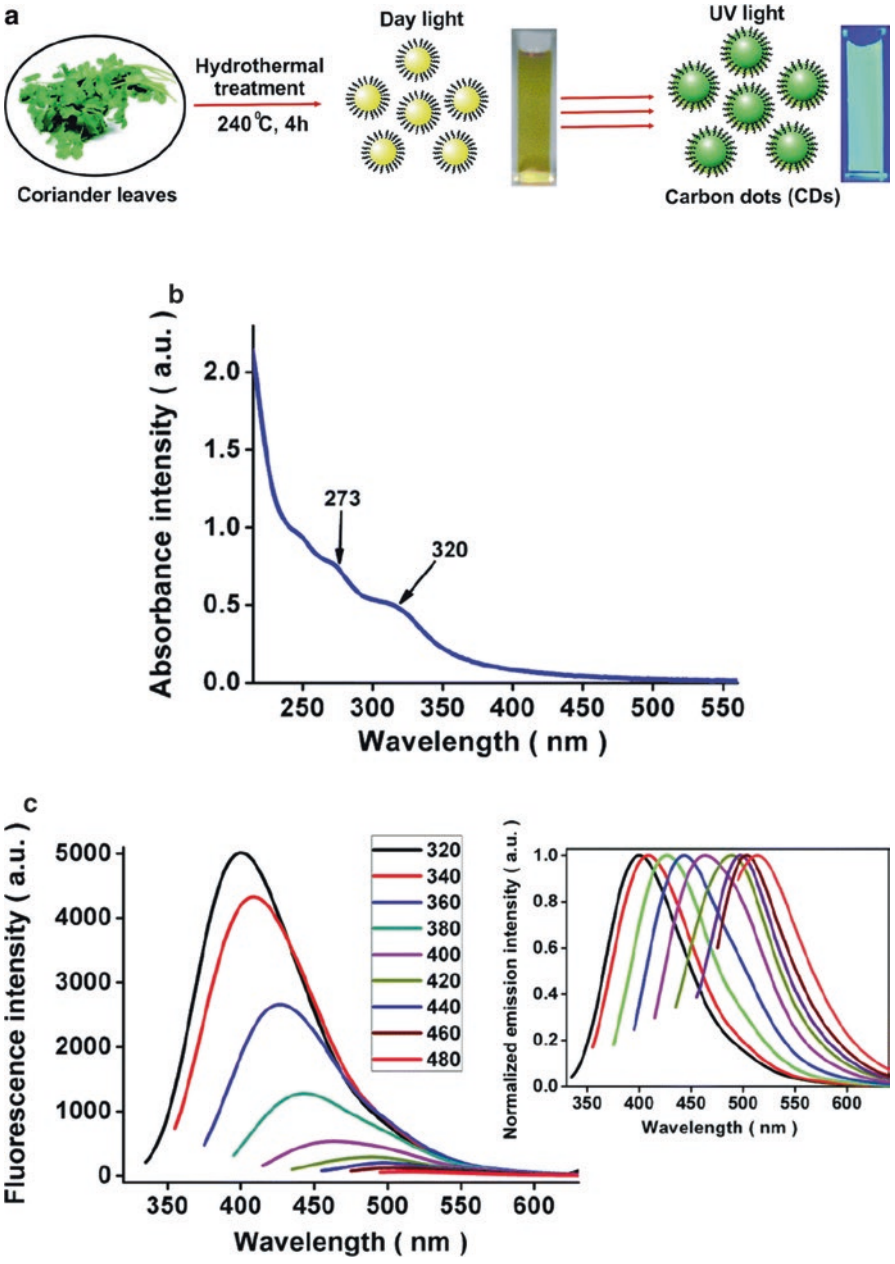

Fig. 1.6 (**a**) Schematic illustration depicting one-step synthesis of CDs from coriander leaves. (**b**) UV-vis absorption spectrum of CDs. (**c**) Fluorescence emission spectra of CDs at different excitation wavelengths ranging from 320 nm to 480 nm with increments of 20 nm (inset: normalized emission intensity). (From Sachdev and Gopinath 2015)

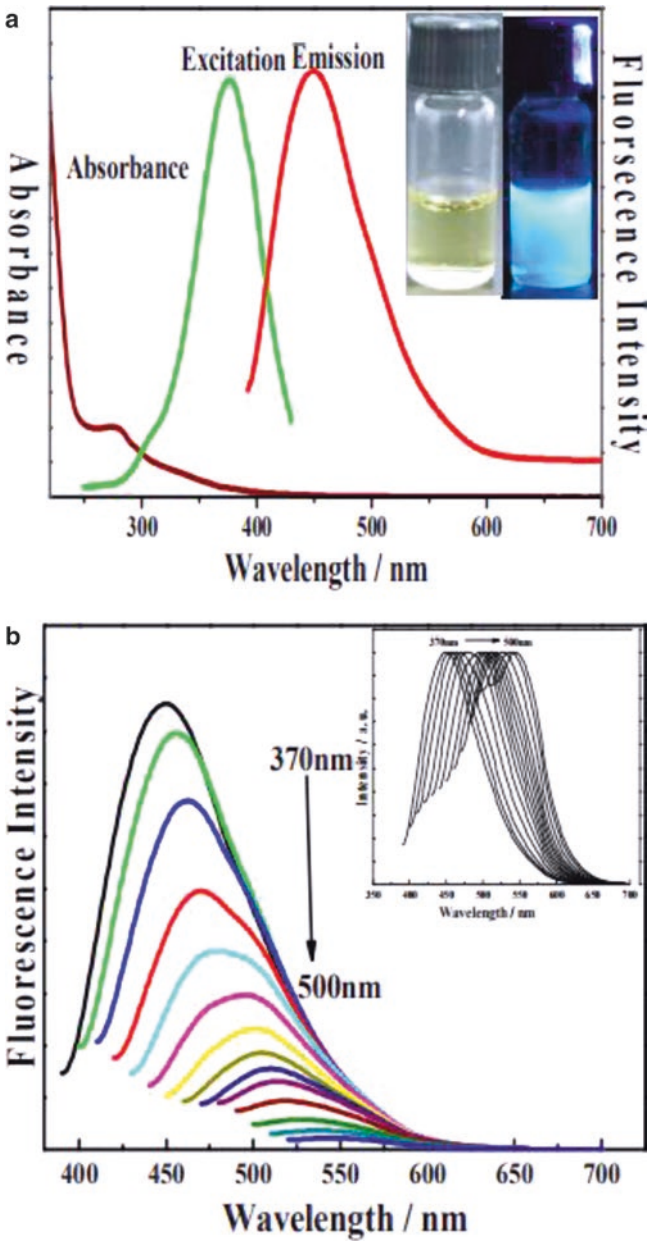

Fig. 1.7 Characteristic optical spectra of CDs. (**a**) UV-vis absorption 10 spectrum and photoluminescent spectra. Inset: photograph taken under daylight (left) and 365 nm UV light (right). (**b**) Emission spectra of CDs recorded for progressively longer excitation wavelength in 10 nm increment from 370 nm to 500 nm. Inset: the normalized PL emission spectra. (From Wu et al. 2013)

et al. 2014). Some researchers observed a maximum absorption peak in the range of 230–278 nm with a tail extending toward the visible region in Fig. 1.7a (Wu et al. 2013; Ramanan et al. 2016; Wei et al. 2014).

1.7.2 Excitation Wavelength-Dependent Fluorescence

The fluorescence emission of CDs depends on the excitation wavelength. Most of the studies show that the maximum emission tends to shift toward higher wavelength with decreasing intensity when the excitation wavelength increases (Figs. 1.6c and 1.7b) (Sachdev and Gopinath 2015; Wu et al. 2013; Liu et al. 2012). This indicates that the emission of CDs could be tuned by altering the excitation wavelength. It was previously reported that the radiative recombinations of the surface-confined electrons and holes contributed to the fluorescence emission of CDs (Cao et al. 2012a; Sk et al. 2014; Zhang et al. 2015). The doping of CDs with nitrogen or sulfur could increase the QY fluorescence due to the formation of new surface states, which trapped the electrons and caused the radiative recombination (Dong et al. 2013). The chemical and electrical structure of CDs is proportionally dependent on the amount of nitrogen and phosphorus doping, thus increasing the fluorescence property of CDs (Zhu et al. 2013). Till now, the origin of the fluorescence of CDs is still not fully understood. Other researchers claimed that this behavior is caused by bond disorder-induced energy gaps (Luo et al. 2009), quantum confinement, and different energy levels associated with surface states arising from the presence of surface functional groups like C-O, C=O, and O=C-OH (Chandra et al. 2012; Bao et al. 2011; Sahu et al. 2012; Li et al. 2011).

1.7.3 Upconverted Photoluminescence (UCPL)

The UCPL properties arise from the multiphotons activation process and cause the simultaneous absorption of two or more photons. Such emission is called anti-Stokes photoluminescence, where the emission wavelength is shorter than the excitation wavelength (Fig. 1.8) (Wang and Hu 2014; Mehta et al. 2014). This feature renders CDs ability to absorb near-infrared light (NIR) and emit UV and visible light which is suitable for the photocatalysis application under sunlight irradiation. A recent work by Sim et al. (2018) found that the sugarcane juice-derived CDs did not exhibit detectable upconversion fluorescence when the excitation wavelength exceeded 540 nm (Fig. 1.9a). Similar results are reported by Wen et al. (2014). They suggested that the frequently obtained UCPL properties could be contributed by the normal fluorescence excited by the leaking component from the second diffraction in the monochromator of the fluorescence spectrophotometer.

1.7.4 Electron Transfer Property

Sim et al. (2018) reported that the incorporation of sugarcane juice-derived CDs into g-C_3N_4 promoted the efficient separation of electron and hole pairs. However, the separation efficiency dropped if the concentration of CDs was excessive

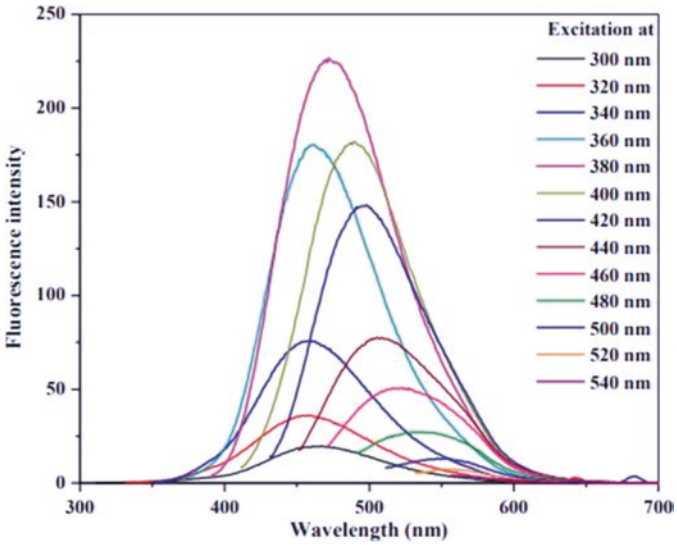

Fig. 1.8 Fluorescence emission spectra of CDs obtained at different excitation wavelengths progressively increasing from 300 nm to 540 nm with a 20 nm increment. (From Mehta et al. 2015)

(Fig. 1.9b). Their work also mentioned that the π-conjugated CDs act as a photosensitizer to sensitize g-C_3N_4 and donate electrons to g-C_3N_4 (Fig. 1.10). The electron transfer property of CDs enables their wide applications in metal ion detection. According to Roshni and Praveen (2017), the electron or energy transfer from CDs surface groups to metal ions like Hg (III) significantly quenched the fluorescence emission of CDs. Such electron transfer process is induced by the presence of hydroxyl and carboxyl or carbonyl groups on the surface of CDs, resulting in the strong binding interaction between the metal ion and these functional groups (Roshni and Praveen 2017; Zhou et al. 2012).

1.8 Applications

CDs have obviously emerged to become an important research field that is still experiencing rapid advances, as reflected by the large number of recent publications. The CDs possess unique features such as tunable fluorescence, easy functionalization, high aqueous solubility, and excellent optical and biological properties which enable their wide applications in different fields. This section summarizes the application of CDs in bioimaging, sensing, photocatalysis, drug delivery, and gene transfer.

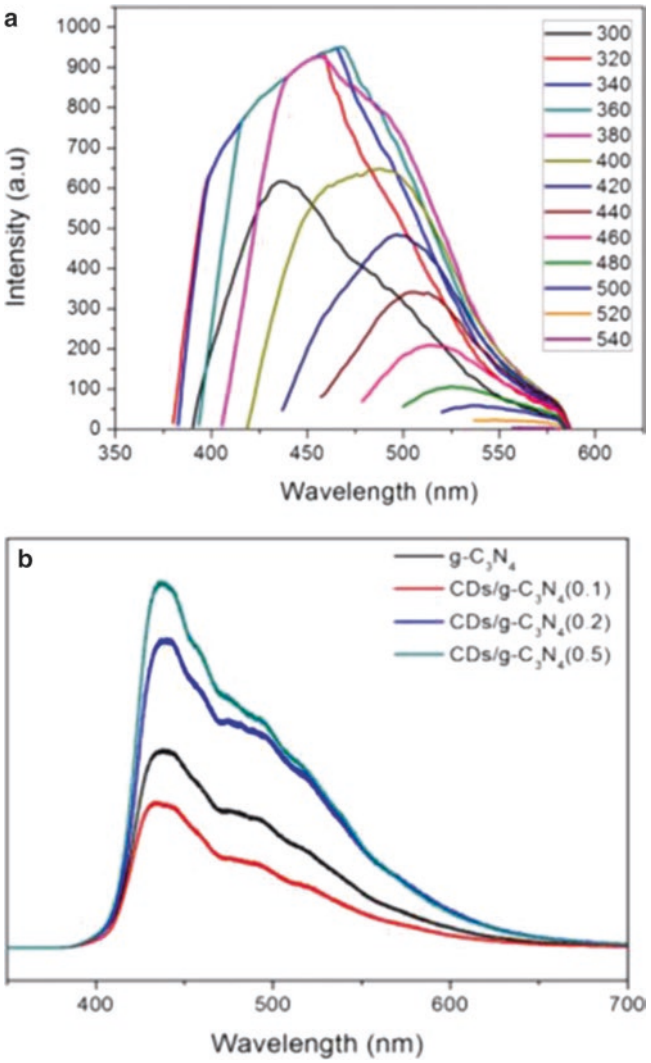

Fig. 1.9 (**a**) The photoluminescence (PL) emission spectrum of CDs at different excitation wavelengths and (**b**) PL spectra of the composites. (From Sim et al. 2018)

1.8.1 Bioimaging

Martynenko et al. (2017) defined that the bioimaging process occurred with labeling of target biomolecule with contrast agent via specific biochemical techniques for read-out system detection. An ideal contrast agent is soluble and stable in suitable buffers or biomatrices and has good analytical signal and photophysics data with

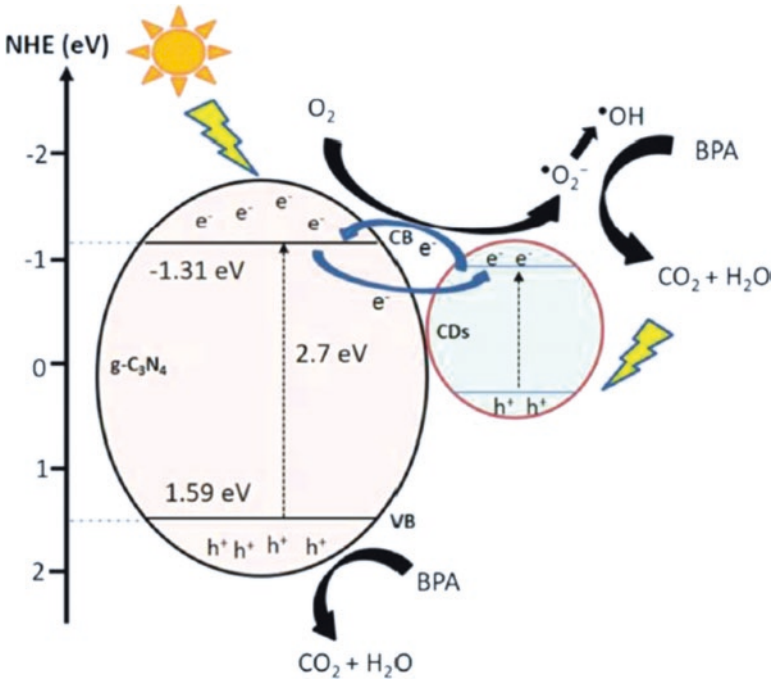

Fig. 1.10 Electron transfer mechanism of CDs/g-C_3N_4. (From Sim et al. 2018)

easy application in practical bioimaging process. CDs were reported to be able to fulfill the requirements as an ideal contrast agent due to their excellent photoluminescence property and biocompatibility to target biomolecule (Peng et al. 2017). The distinctive advantages of CDs in bioimaging such as excellent photostability, multicolor emission profile, and small size were also described by Zhang and Yu (2015). Fluorescent CDs derived from 2-propanol in Angamuthu et al.'s (2018) study showed clear zone of HeLa cell nuclei upon excitation of 488 nm wavelength in confocal microscopy imaging. The 2-propanol-derived CDs also exhibited low cytotoxicity and positive biocompatibility upon HeLa cell incubation which conformed to the advantages of CDs. Another research by Lin et al. (2014) demonstrated that the CDs synthesized from shrimp eggs exhibited blue, green, and red fluorescences at cell membrane and cytoplasm of SK-Hep-1 cells upon delivery for 24 h, shown in Fig. 1.11. The multicolor emission of CDs performed better in bioimaging application compared with traditional fluorescent protein with single fluorescence characteristic. Yang et al.'s (2009) study was able to develop highly fluorescent CDs as prominent contrast agent for optical imaging in vivo for the first time. The PEGylated CDs was injected subcutaneously into female mice and imagined in Lumazone FA in vivo imaging system with 470 nm and 525 nm emission filters. Figure 1.12 shows the intravenous injection of CDs into the mice. It was demonstrated that the fluorescence from CDs was readily detected in urine which

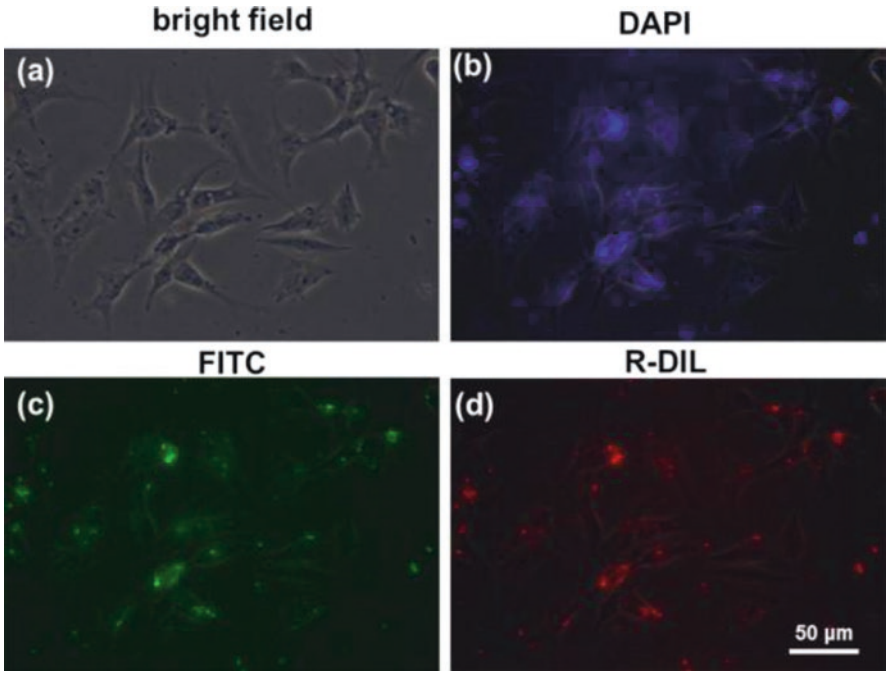

Fig. 1.11 Images of bright-field and fluorescence images of SK-Hep-1 cells treated with CDs derived from shrimp eggs. (From Lin et al. 2014)

suggested urine excretion of CDs from the mice body after 3 h postinjection. This deduced that the CDs would be excreted after injection which reduced its toxicity in the mice. Furthermore, Cao et al. (2012) also confirmed Yang et al. (2009) report of applied CDs in mice for bioimaging. They presented that fluorescence signals of CDs injected in subcutaneous layer of female mice would diffuse and fade slowly within 24 h. The CDs also migrated along the arm of mice with consistent fluorescent emission. Cao et al. (2012) also compared with conventional CdSe/ZnS QDs in bioimaging of mice and discovered that the resulting fluorescence images of both CDs and CdSe/ZnS QDs were similar in brightness and fluorescent quantum yields. However, CDs had a better advantage compared with CdSe/ZnS QDs as it is nontoxic to the mice.

1.8.2 Sensing

Han et al. (2017) stated that the sensing based on fluorescence had received huge attention due to its excellent sensitivity, low cost, and short response time. The fluorescence sensing mechanism involved four different mechanisms such as photoinduced electron transport (PET), resonance energy transfer (RET), photoinduced

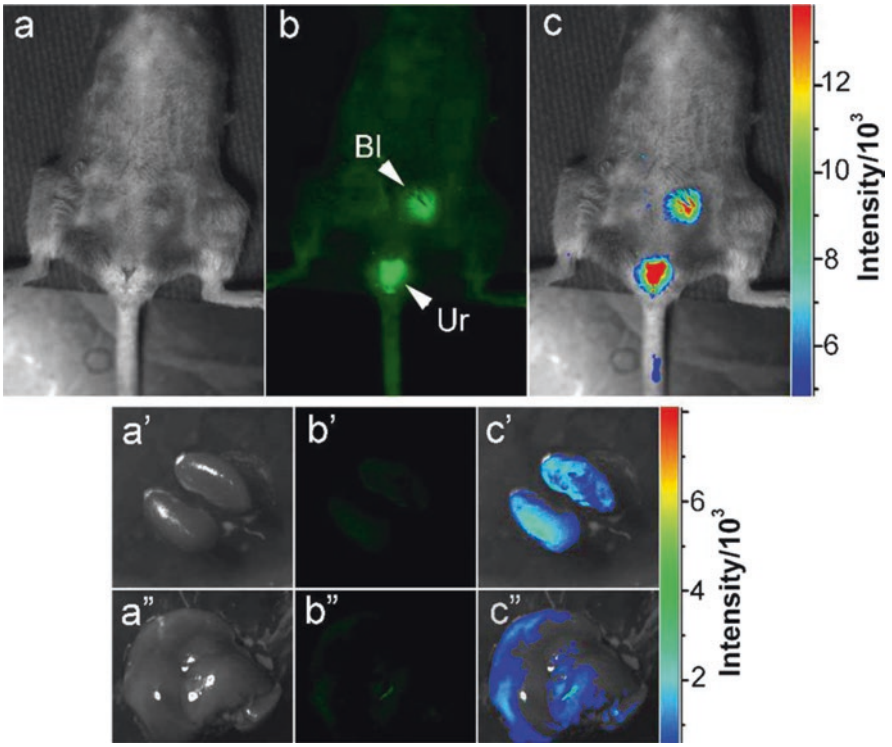

Fig. 1.12 Intravenous injection of (**a**) bright field, (**b**) as-detected fluorescence (Bl (bladder) and Ur (urine)), and (**c**) color-coded images. Similar order for the images of the dissected kidneys at the lower left and liver at lower right. (From Yang et al. 2009)

charge transfer (PCT), and inner filter effect (IFE) (Sun and Lei 2017). The PET process involved the internal redox reaction, while RET used long-range dipolar interaction between excited state of CDs and another species to produce fluorescence emission. In addition, PCT mechanism transfer electrons from electron donor to acceptor in partial charge transfer of fully conjugated π system. The IFE process differed from the rest of the mechanism as this mechanism utilized quenching, which allowed fluorescence lifetime to be independent of total intensity. CDs can be used as an effective sensing agent as it is abundant, benign, and low cost. In comparison with other traditional semiconductor QDs, CDs had higher solubility, chemical inertness, resistance toward photobleaching, and facile modification. Han et al. (2018) described that the synthesized CDs with various functional group were able to detect multiple compounds such as hydrogen peroxide, glutathione, mercury ion (Hg^{2+}), silver ion (Ag^{+}), tetracycline, and enrofloxacin hydrochloride. Furthermore, the fungus-derived CDs were able to recover 105.0% of hyaluronidase in human urine (Yang et al. 2017). Hyalurondase is an enzyme that degraded hyaluronic acid and had been recognized as a new tumor marker type which allowed the fungus-derived CDs to detect tumor in human body. Li et al. (2017) also reported

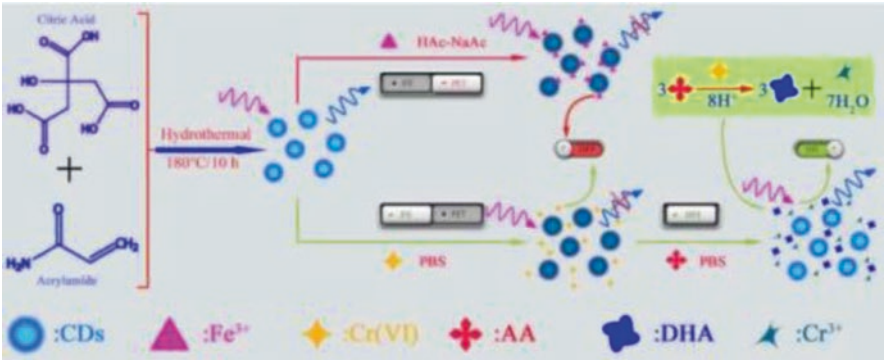

Fig. 1.13 Hydrothermally synthesized CDS in three sensing modes for Fe^{3+}, Cr (VI), and ascorbic acid via different methods including PET, IFE, and elimination IFE mechanism type. (From Li et al. 2017)

hydrothermally synthesized CDs were able to detect iron ion (Fe^{3+}), chromium (Cr(VI)) ion, and ascorbic acid in lake water and industrial water via PET, IFE, and elimination IFE mechanisms. These mechanisms were shown in Fig. 1.13. Fluorescent CDs produced from carnation in Zhong et al. (2016) exhibited colorimetric response from pH ranging from 12.8 to 4.6 and under different light sources of daylight and UV light. The fluorescent CDs that corresponded to the different pH values showed that CDs act as a colorimetric and fluorescent sensor for pH sensing. Hematin that bound to the membrane of red cell and caused any related sickle-cell anemia was sensed by p-aminobenzoic acid-synthesized CDs in human blood sample using IFE (Zhang et al. 2018). Therefore, the CDs were able to distinguish hematin from complex solution and act as good and stable as fluorescence nanoprobe.

1.8.3 Biomedicine (Drug Delivery and Gene Transfer)

The fluorescence property of CDs had allowed the application of biomedicine in targeted drug delivery and gene therapy owing to their aqueous solubility, facile synthesis, and quantum yield (Jaleel and Pramod 2017). Drug delivery significantly determined the therapeutic efficiency and nonproductive distribution of specific treatments. Yuan et al. (2017) detailed that the chemotherapeutics with reduced drug delivery can lead to increase drug dosages and undesirable side effects during treatment. CDs were able to aid the chemotherapeutic treatment as they exhibit superb loading, release, target, and tracking of drug properties. Carrot root-derived CDs were reported by D'souza et al. (2018) to effectively hold and deliver mitomycin drug to cancer cell due to their biocompatibility and ultrasmall size. The green-synthesized CDs acted as optimal drug vehicles by offering excellent selectivity and specificity for mitomycin drug delivery system development. Feng et al. (2016)

described that the modification of single surface property of CDs formed charge-convertible property in mildly acidic tumor extracellular microenvironment at approximately pH 6.8. The CDs with the addition of polyethylene glycol allowed pH-responsive characteristics by changing the charge to negative at normal physiological environment at pH 7.4 and reverse to positive charge at tumor extracellular microenvironment. These properties allowed the CDs to have a prolonged blood circulation time, enhanced permeability and retention (EPR) effect, enhanced tumor cell internalization, less side effects at normal physiological condition, improved endosome escape, and controlled cytotoxic release of cisplatin, an anticancer drug in cancer cell as shown in Fig. 1.14.

Alternatively, the high photoluminescence property allowed the CDs to act as a promising probe for gene therapy. The gene therapy developed gene carriers which were initially done via virus. Viruses were effective transfection vectors but had issues with carcinogenicity, immunogenicity, and ammation. Therefore, CDs were developed to overcome virus limitation as CDs had high transfection efficiency and low toxicity (Yang et al. 2017). Sodium alginate-derived CDs were synthesized and acted as a gene vector for plasmid TGF-β1 delivery in Zhou et al.'s (2016) study. The green CDs were compared with Lipofectamine 2000, branched PEI, and semiconductor QDs in transfection efficiency, and the results showed that the CDs had a higher transfection efficiency due to its low toxicity, small size, positive surface charge, and strong condensation effect on pDNA macromolecule that prevented pDNA enzymolysis. Zhang et al. (2016) stated that the fluorescent CDs with small interfering RNA (siRNA) conjugate were able to deliver 1/30 of siRNA amount in comparative with gold nanoparticles. The fluorescent CDs-based siRNA conjugate

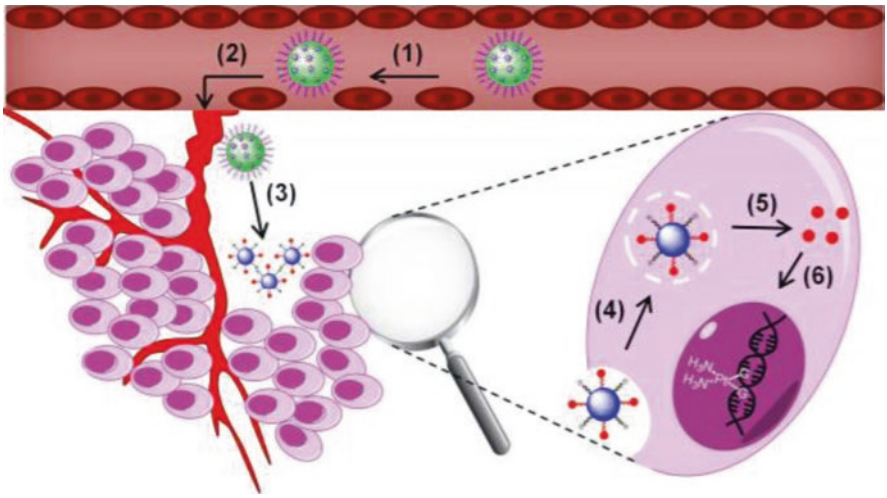

Fig. 1.14 Illustration for the drug delivery process of CDs-modified polyethylene glycol: (1) prolonged blood circulation time, (2) enhanced permeability and retention (EPR) effect, (3) enhanced tumor cell internalization, (4) less side effects at normal physiological condition, (5) improved endosome escape, and (6) controlled cytotoxic release of cisplatin, an anticancer drug in cancer cell. (From Feng et al. 2016)

reduced approximately 80% of A375 cells via cellular Plk1 mRNA treatment which led to induce apoptosis in 31.90% of A375 cells and 20.33% of MCF-7 cells. These apoptosis induction efficiency was higher than commercially available Lipofectamine 200, which further proved the efficiency of CDs-based siRNA conjugate in gene delivery and therapy.

1.8.4 Photocatalysis

Han et al. (2018) described that photocatalysis involved the synergistic effect of light and catalyst during energy conversion material process which degraded contaminates and obtained hydrogen energy. An ideal photocatalyst for photocatalysis process should have a wide light absorption range and high photogenerated charge carrier separation efficiency for enhanced overall quantum efficiency and practical applications. Photocatalysis process can be utilized in water splitting technologies which generate hydrogen generation and pollutant removal remediation methods. CDs were able to produce photogenerated charge carriers under light irradiation and had unique properties of low cost, excellent photoelectric properties, enhanced adsorption capacity, and nontoxic nature. Besides that, CDs were reported by Yu et al. (2016) to be a viable alternative in comparison to the expensive platinum group metal-modified photocatalyst as CDs had an intrinsic bandgap owing to quantum confinement and edge effect which enhanced the separation of photogenerated charge carrier (Lu et al. 2016). As reported by Yang et al. (2015), pure CDs produced without any modification and co-catalyst generated hydrogen from pure water at a higher rate of 34.8 times compared with commercial TiO_2 Degussa P25 when methanol was utilized as the sacrificial reagent. The enhanced photocatalytic ability of pure CDs in water splitting was due to CDs big band gap, low photoluminescence intensity, strong oxidation and reduction potential which ultimately, lowered the recombination rate of photogenerated charge carriers and increased the photocatalytic activities. For optimization of photocatalytic process, the CDs were required to adopt two material design approaches such as the band alignment and interfacial properties manipulation and properties tuning on heteroatom doping, particle size and surface state. The first approach of band alignment manipulation was difficult to be achieved singly as the highest unoccupied molecular orbital (HOMO) and lowest unoccupied molecular orbital (LUMO) was governed by size and shape factors. Hu et al. (2016) explained that the doping of heteroatom in CDs was able to tailor the charge distribution of CDs surface which facilitate better photogenerated charge carrier separation. The synthesized chlorine (Cl) and phosphorus (P) functionalized CDs showed higher photocatalytic efficiency in methylene blue and methyl orange dye under visible light irradiation. Another study done by Sim et al. (2018) showed that the CDs and graphitic carbon nitride ($g\text{-}C_3N_4$) composite completely degraded Bisphenol A (BPA) pollutant after 90 min under solar irradiation due to its superb visible light absorption capability. The approach of CDs application in photocatalytic treatment of recalcitrant pollutant would prove to be a renewable and sustainable method for future treatments.

References

Alam A, Park BY, Ghouri ZK, Park M, Kim HY (2015) Synthesis of carbon quantum dot from cabbage with down and up-conversion photoluminescence properties: excellent imaging agent for biomedical application. Green Chem 17:3791–3797

Angamuthu R, Palanisamy P, Vasudevan V, Nagarajan S, Rajendran R, Vairamuthu R (2018) Quick synthesis of 2-propanol derived fluorescent carbon dots for bioimaging applications. Opt Mater 78:477–483

Anmei S, Qingmei Z, Yuye C, Yilin W (2018) Preparation of carbon quantum dots from cigarette filters and its application for fluorescence detection of Sudan I. Anal Chim Acta 1023:115–120

Arora N, Sharma NN (2014) Arc discharge synthesis of carbon nanotubes: comprehensive review. Diam Relat Mater 50:135–150

Arumugam N, Kim J (2018) Synthesis of carbon quantum dots from broccoli and their ability to detect silver ions. Mater Lett 219:37–40

Baker SN, Baker GA (2010) Luminescent carbon nanodots: emergent nanolights. Angew Chem Int Ed 49:6726–6744

Bandi R, Gangapuram BR, Dadigala R, Eslavath R, Singh SS, Guttena V (2016) Facile and green synthesis of fluorescent carbon dots from onion waste and their potential applications as sensor and multicolour imaging agents. RSC Adv 6:28633–28639

Bao L, Zhang ZL, Tian ZQ, Zhang L, Liu C, Lin Y, Qi B, Pang DW (2011) Electrochemical tuning of luminescent carbon nanodots: from preparation to luminescence mechanism. Adv Mater 23:5801–5806

Bottini M, Balasubramanian C, Dawson MI, Bergamaschi A, Bellucci S, Mustelin T (2006) Isolation and characterization of fluorescent nanoparticles from pristine and oxidized electric arc-produced single-walled carbon nanotubes. J Phys Chem B 110:831–836

Cachier H, Bremond MP, Buat-Ménard P (1989) Determination of atmospheric soot carbon with a simple thermal method. Tellus B 41:379–390

Cao L, Yang ST, Wang X, Luo PG, Liu JH, Sahu S, Liu Y, Sun YP (2012) Competitive performance of carbon "quantum" dots in optical bioimaging. Theranostics 2:295

Cao LI, Meziani MJ, Sahu S, Sun YP (2012a) Photoluminescence properties of graphene versus other carbon nanomaterials. Acc Chem Res 46:171–180

Chandra S, Pathan SH, Mitra S, Modha BH, Goswami A, Pramanik P (2012) Tuning of photoluminescence on different surface functionalized carbon quantum dots. RSC Adv 2:3602–3606

Choi Y, Thongsai N, Chae A, Jo S, Kang EB, Paoprasert P, Park SY, In I (2017) Microwave-assisted synthesis of luminescent and biocompatible lysine-based carbon quantum dots. Ind Eng Chem Res 47:329–335

D'souza SL, Deshmukh B, Rawat KA, Bhamore JR, Lenka N, Kailasa SK (2016) Fluorescent carbon dots derived from vancomycin for flutamide drug delivery and cell imaging. New J Chem 40:7075–7083

D'souza SL, Chettiar SS, Koduru JR, Kailasa SK (2018) Synthesis of fluorescent carbon dots using *Daucus carota subsp. sativus* roots for mitomycin drug delivery. Optik 158:893–900

De B, Karak N (2013) A green and facile approach for the synthesis of water soluble fluorescent carbon dots from banana juice. RSC Adv 3:8286–8290

Demchenko AP, Dekaliuk MO (2013) Novel fluorescent carbonic nanomaterials for sensing and imaging. Methods Appl Fluoresc 1:042001

Deng J, Lu Q, Mi N, Li H, Liu M, Xu M, Tan L, Xie Q, Zhang Y, Yao S (2014) Electrochemical synthesis of carbon nanodots directly from alcohols. Chem Eur J 20:4993–4999

Ding H, Ji Y, Wei JS, Gao QY, Zhou ZY, Xiong HM (2017) Facile synthesis of red-emitting carbon dots from pulp-free lemon juice for bioimaging. J Mater Chem B 5:5272–5277

Dong Y, Zhou N, Lin X, Lin J, Chi Y, Chen G (2010) Extraction of electrochemiluminescent oxidized carbon quantum dots from activated carbon. Chem Mater 22:5895–5899

Dong Y, Pang H, Yang HB, Guo C, Shao J, Chi Y, Li CM, Yu T (2013) Carbon-based dots co-doped with nitrogen and sulfur for high quantum yield and excitation-independent emission. Angew Chem Int Ed 52:7800–7804

Du FY, Zhang MM, Li XF, Li JN, Jiang XY, Li Z, Hua Y, Shao GB, Jin J, Shao QX, Zhou M, Gong AH (2014) Economical and green synthesis of bagasse derived fluorescent carbon dots for biomedical applications. Nanotechnology 25:315702–315712

Essner JB, Laber CH, Ravula S, Polo-Parada L, Baker GA (2016) Pee-dots: biocompatible fluorescent carbon dots derived from the upcycling of urine. Green Chem 18:243–250

Fadllan A, Marwoto P, Aji MP, Susanto, Iswari RS (2017) Synthesis of carbon nanodots from waste paper with hydrothermal method. AIP Publishing 1788:030069

Fan RJ, Sun Q, Zhang L, Zhang Y, Lu AH (2014) Photoluminescent carbon dots directly derived from polyethylene glycol and their application for cellular imaging. Carbon 71:87–93

Feng T, Ai X, An G, Yang P, Zhao Y (2016) Charge-convertible carbon dots for imaging-guided drug delivery with enhanced in vivo cancer therapeutic efficiency. ACS Nano 10:4410–4420

Gonçalves H, Jorge PA, Fernandes JRA, da Silva JCE (2010) Hg (II) sensing based on functionalized carbon dots obtained by direct laser ablation. Sensors Actuators B Chem 145:702–707

Gondal MA, Qahtan TF, Dastageer MA, Saleh TA, Maganda YW, Anjum DH (2013) Effects of oxidizing medium on the composition, morphology and optical properties of copper oxide nanoparticles produced by pulsed laser ablation. Appl Surf Sci 286:149–155

Guo YM, Zhang LF, Cao FP, Leng YM (2016) Thermal treatment of hair for the synthesis of sustainable carbon quantum dots and the applications for sensing Hg^{2+}. Sci Rep 6:35795

Guo L, Li L, Liu M, Wan Q, Tian J, Huang Q, Wen Y, Liang S, Zhang X, Wei Y (2017) Bottom-up preparation of nitrogen doped carbon quantum dots with green emission under microwave-assisted hydrothermal treatment and their biological imaging. Mater Sci Eng C 84:60–66

Han M, Zhu S, Lu S, Song Y, Feng T, Tao S, Liu J, Yang B (2018) Recent progress on the photocatalysis of carbon dots: classification, mechanism and applications. Nano Today 19:201–208

Hossain MA, Islam S (2013) Synthesis of carbon nanoparticles from kerosene and their characterization by SEM/EDX, XRD and FTIR. J Nanosci Nanotechnol 1:52–56

Hou Y, Lu Q, Deng J, Li H, Zhang Y (2015) One-pot electrochemical synthesis of functionalized fluorescent carbon dots and their selective sensing for mercury ion. Anal Chim Acta 866:69–74

Hu B, Wang K, Wu L, Yu SH, Antonietti M, Titirici MM (2010) Engineering carbon materials from the hydrothermal carbonization process of biomass. Adv Mater 22:813–828

Hu S, Chang Q, Lin K, Yang J (2016) Tailoring surface charge distribution of carbon dots through heteroatoms for enhanced visible-light photocatalytic activity. Carbon 105:484–489

Huang H, Lv JJ, Zhou DL, Bao N, Xu Y, Wang AJ, Feng JJ (2013) One-pot green synthesis of nitrogen-doped carbon nanoparticles as fluorescent probes for mercury ions. RSC Adv 3:21691–21696

Jaleel JA, Pramod K (2017) Artful and multifaceted applications of carbon dot in biomedicine. J Control Release 269:302–321

Jelinek R (2017) Carbon quantum dots: synthesis, properties and applications. Springer International Publishing AG, Cham

Ju E, Liu Z, Du Y, Tao Y, Ren J, Qu X (2014) Heterogeneous assembled nanocomplexes for ratiometric detection of highly reactive oxygen species in vitro and in vivo. ACS Nano 8:6014–6023

Jia Zhang, Shu-Hong (2016) Carbon dots: large-scale synthesis, sensing and bioimaging. Mater Today 19(7):382–393

Kasibabu BSB, D'souza SL, Jha S, Kailasa SK (2015) Imaging of bacterial and fungal cells using fluorescent carbon dots prepared from *Carica Papaya* juice. J Fluoresc 25:803–810

Kazemizadeh F, Malekfar R, Parvin P (2017) Pulsed laser ablation synthesis of carbon nanoparticles in vacuum. J Phys Chem Solids 104:252–256

Kshirsagar A, Khanna T, Khanna P, Dhanwe V, Khanna PK (2017) Flame deposition method for carbon nanoparticles employing green precursors and its composite with Au nanoparticles for photocatalytic degradation of methylene blue. Vacuum 146:633–640

Kumar A, Ray A, Laha D, Kumar T, Karmakar P, Kumar S (2017) Chemical green synthesis of carbon dots from *Ocimum Sanctum* for effective fluorescent sensing of Pb^{2+} ions and live cell imaging. Sensors Actuators B Chem 242:679–686

Li H, He X, Kang Z, Huang H, Liu Y, Liu J, Lian S, Tsang CHA, Yang X, Lee ST (2010) Water-soluble fluorescent carbon quantum dots and photocatalyst design. Angew Chem Int Ed 49:4430–4434

Li X, Wang H, Shimizu Y, Pyatenko A, Kawaguchi K, Koshizaki N (2011) Preparation of carbon quantum dots with tunable photoluminescence by rapid laser passivation in ordinary organic solvents. Chem Commun 47:932–934

Li W, Yue Z, Wang C, Zhang W, Liu G (2013) An absolutely green approach to fabricate carbon nanodots from soya bean grounds. RSC Adv 3:20662–20665

Li C, Liu W, Sun X, Pan W, Wang J (2017) Multi sensing functions integrated into one carbon-dot based platform via different types of mechanisms. Sensors Actuators B Chem 252:544–553

Liang F, Tanaka M, Choi S, Watanabe T (2017) Formation of different arc-anode attachment modes and their effect on temperature fluctuation for carbon nanomaterial production in DC arc discharge. Carbon 117:100–111

Liao J, Cheng Z, Zhou L (2016) Nitrogen-doping enhanced fluorescent carbon dots: green synthesis and their applications for bioimaging and label-free detection of Au^{3+} ions. ACS Sustain Chem Eng 4:3053–3061

Lim S, Shen W, Gao Z (2015) Carbon quantum dots and their applications. Chem Soc Rev 44:362–381

Lin PY, Hsieh CW, Kung ML, Chu LY, Huang HJ, Chen HT, Wu DC, Kuo CH, Hsieh SL, Hsieh S (2014) Eco-friendly synthesis of shrimp egg-derived carbon dots for fluorescent bioimaging. J Biotechnol 189:114–119

Liu S, Tian JQ, Wang L, Zhang YW, Qin XY, Luo YL, Asiri AM, Al-Youbi AO, Sun XP (2012) Hydrothermal treatment of grass: a low-cost, green route to nitrogen-doped, carbon-rich, photoluminescent polymer nanodots as an effective fluorescent sensing platform for label-free detection of Cu(II) ions. Adv Mater 24:2037–2041

Liu X, Pang J, Xu F, Zhang X (2016) Simple approach to synthesize amino-functionalized carbon dots by carbonization of chitosan. Sci Rep 6:31100

Liu F, Zhang W, Chen W, Wang J, Yang Q, Zhu W, Wang J (2017) One-pot synthesis of $NiFe_2O_4$ integrated with EDTA-derived carbon dots for enhanced removal of tetracycline. Chem Eng J 310:187–196

Liu W, Diao H, Chang H, Wang H, Li T, Wei W (2017a) Green synthesis of carbon dots from rose-heart radish and application for Fe^{3+} detection and cell imaging. Sensors Actuators B Chem 241:190–198

Lu WB, Qin XY, Liu S, Chang GH, Zhang YW, Luo YL, Asiri AM, Al-Youbi AO, Sun XP (2012) Economical, green synthesis of fluorescent carbon nanoparticles and their use as probes for sensitive and selective detection of mercury(II) ions. Anal Chem 84:5351–5357

Lu W, Qin X, Asiri AM, Al-Youbi AO, Sun X (2013) Green synthesis of carbon nanodots as an effective fluorescent probe for sensitive and selective detection of mercury (II) ions. J Nanopart Res 15:1344

Lu KQ, Quan Q, Zhang N, Xu YJ (2016) Multifarious roles of carbon quantum dots in heterogeneous photocatalysis. J Energy Chem 25:927–935

Luo Z, Vora PM, Mele EJ, Johnson AC, Kikkawa JM (2009) Photoluminescence and band gap modulation in graphene oxide. Appl Phys Lett 94:111909

Ma Z, Ming H, Huang H, Liu Y, Kang Z (2012) One-step ultrasonic synthesis of fluorescent N-doped carbon dots from glucose and their visible-light sensitive photocatalytic ability. New J Chem 36:861–864

Martynenko IV, Litvin AP, Purcell-Milton F, Baranov AV, Fedorov AV, Gun'ko YK (2017) Application of semiconductor quantum dots in bioimaging and biosensing. J Mater Chem B 5:6701–6727

Mehta VN, Jha S, Kailasa SK (2014) One-pot green synthesis of carbon dots by using *Saccharum officinarum* juice for fluorescent imaging of bacteria (*Escherichia coli*) and yeast (*Saccharomyces cerevisiae*) cells. Mater Sci Eng C 38:20–27

Mehta VN, Jha S, Basu H, Singhal RK, Kailasa SK (2015) One-step hydrothermal approach to fabricate carbon dots from apple juice for imaging of mycobacterium and fungal cells. Sensors Actuators B Chem 213:434–443

Menéndez JA, Arenillas A, Fidalgo B, Fernández Y, Zubizarreta L, Calvo EG, Bermúdez JM (2010) Microwave heating processes involving carbon materials. Fuel Process Technol 91:1–8

Ming H, Ma Z, Liu Y, Pan K, Yu H, Wang F, Kang Z (2012) Large scale electrochemical synthesis of high quality carbon nanodots and their photocatalytic property. Dalton Trans 41:9526–9531

Mumei Han, Liping Wang, Siheng Li, Liang Bai, Yunjie Zhou, Yue Sun, Hui Huang, Hao Li, Yang Liu, Zhenhui Kang (2017) High-bright fluorescent carbon dot as versatile sensing platform. Talanta 174:265–273

Namdari P, Negahdari B, Eatemadi A (2017) Synthesis, properties and biomedical applications of carbon-based quantum dots : an updated review. Biomed Pharmacother 87:209–222

Nersisyan HH, Lee JH, Ding JR, Kim KS, Manukyan KV, Mukasyan AS (2017) Combustion synthesis of zero-, one-, two-and three-dimensional nanostructures: current trends and future perspectives. Prog Energy Combust Sci 63:79–118

Pandey S, Shah R, Mewada A, Thakur M, Oza G, Sharon M (2013) Gold nanorods mediated controlled release of doxorubicin: nano-needles for efficient drug delivery. J Mater Sci Mater Med 24:1671–1681

Park SY, Lee HU, Park ES, Lee SC, Lee JW, Jeong SW, Kim CH, Lee YC, Huh YS, Lee J (2014) Photoluminescent green carbon nanodots from food-waste-derived sources: large-scale synthesis, properties, and biomedical applications. ACS Appl Mater Interfaces 6:3365–3370

Peng Z, Han X, Li S, Al-Youbi AO, Bashammakh AS, El-Shahawi MS, Leblanc RM (2017) Carbon dots: biomacromolecule interaction, bioimaging and nanomedicine. Coord Chem Rev 343:256–277

Pham-Truong TN, Petenzi T, Ranjan C, Randriamahazaka H, Ghilane J (2018) Microwave assisted synthesis of carbon dots in ionic liquid as metal free catalyst for highly selective production of hydrogen peroxide. Carbon 130:544–552

Prasannan A, Imae T (2013) One-pot synthesis of fluorescent carbon dots from orange waste peels. Ind Eng Chem Res 52:15673–15678

Qin XY, Lu WB, Asiri AM, Al-Youbi AO, Sun XP (2012) Green, low-cost synthesis of photoluminescent carbon dots by hydrothermal treatment of willow bark and their application as an effective photocatalyst for fabricating Au nanoparticles/reduced graphene oxide nanocomposites for glucose detection. Cat Sci Technol 3:1027–1035

Rahy A, Zhou C, Zheng J, Park SY, Kim MJ, Jang I, Cho SJ, Yang DJ (2012) Photoluminescent carbon nanoparticles produced by confined combustion of aromatic compounds. Carbon 50:1298–1302

Ramanan V, Thiyagarajan SK, Raji K, Suresh R, Sekar R, Ramamurthy P (2016) Outright green synthesis of fluorescent carbon dots from eutrophic algal blooms for in vitro imaging. ACS Sustain Chem Eng 4:4724–4731

Roshni V, Praveen OD (2017) Fluorescent N-doped Carbon Dots from Mustard Seeds: One step Green Synthesis and its Application as an effective Hg (II) Sensor. Braz J Anal Chem 4(14):17–24

Sachdev A, Gopinath P (2015) Green synthesis of multifunctional carbon dots from coriander leaves and their potential application as antioxidants, sensors and bioimaging agents. Analyst 140:4260–4269

Sachdev A, Matai I, Kumar SU, Bhushan B, Dubey P, Gopinath P (2013) A novel one-step synthesis of PEG passivated multicolour fluorescent carbon dots for potential biolabeling application. RSC Adv 3:16958–16961

Sachdev A, Matai I, Gopinath P (2014) Implications of surface passivation on physicochemical and bioimaging properties of carbon dots. RSC Adv 4:20915–20921

Sahu S, Behera B, Maiti TK, Mohapatra S (2012) Simple one-step synthesis of highly luminescent carbon dots from orange juice: application as excellent bio-imaging agents. Chem Commun 48:8835–8837

Schneider J, Reckmeier CJ, Xiong Y, von Seckendorff M, Susha AS, Kasák P, Rogach AL (2017) Molecular fluorescence in citric acid-based carbon dots. J Phys Chem C 121:2014–2022

Shahidi S, Rashidian M, Dorranian D (2018) Preparation of antibacterial textile using laser ablation method. Opt Laser Technol 99:145–153

Sharma V, Tiwari P, Mobin SM (2017) Sustainable carbon-dots: recent advances in green carbon dots for sensing and bioimaging. J Mater Chem B 5:8904–8924

Shen LM, Liu J (2016) New development in carbon quantum dots technical applications. Talanta 156-157:245–256

Sim LC, Wong JL, Hak CH, Tai JY, Leong KH, Saravanan P (2018) Sugarcane juice derived carbon dot–graphitic carbon nitride composites for bisphenol A degradation under sunlight irradiation. Beilstein J Nanotechnol 9:353–363

Sk MA, Ananthanarayanan A, Huang L, Lim KH, Chen P (2014) Revealing the tunable photoluminescence properties of graphene quantum dots. J Mater Chem C 2:6954–6960

Štěpánková S, Kozák O, Zbořil R (2015) Surfactant-based fluorescent quantum carbon dots: synthesis and application. Adv Mater Res 1088:381–385

Sun X, Lei Y (2017) Fluorescent carbon dots and their sensing applications. Trends Anal Chem 89:163–180

Sun YP, Zhou B, Lin Y, Wang W, Fernando KS, Pathak P, Meziani MJ, Harruff BA, Wang X, Wang H, Luo PG (2006) Quantum-sized carbon dots for bright and colorful photoluminescence. J Am Chem Soc 128:7756–7757

Sun D, Ban R, Zhang PH, Wu GH, Zhang JR, Zhu JJ (2013) Hair fiber as a precursor for synthesizing of sulfur-and nitrogen-co-doped carbon dots with tunable luminescence properties. Carbon 64:424–434

Sun DL, Hong RY, Wang F, Liu JY, Kumar MR (2016) Synthesis and modification of carbon nanomaterials via AC arc and dielectric barrier discharge plasma. Chem Eng J 283:9–20

Tian L, Ghosh D, Chen W, Pradhan S, Chang X, Chen S (2009) Nanosized carbon particles from natural gas soot. Chem Mater 21:2803–2809

Wang Y, Hu A (2014) Carbon quantum dots: synthesis, properties and applications. J Mater Chem C 2:6921–6939

Wang L, Zhou HS (2014) Green synthesis of luminescent nitrogen-doped carbon dots from milk and its imaging application. Anal Chem 86:8902–8905

Wang X, Cao L, Lu FS, Meziani MJ, Li HT, Qi G, Zhou B, Harruff BA, Kermarrec F, Sun YP (2009) Photoinduced electron transfers with carbon dots. Chem Commun 25:3774–3776

Wang X, Maeda K, Thomas A, Takanabe K, Xin G, Carlsson JM, Domen K, Antonietti M (2009a) A metal-free polymeric photocatalyst for hydrogen production from water under visible light. Nat Mater 8:76–80

Wang Q, Zheng H, Long Y, Zhang L, Gao M, Bai W (2011) Microwave–hydrothermal synthesis of fluorescent carbon dots from graphite oxide. Carbon 49:3134–3140

Wang J, Wang CF, Chen S (2012) Amphiphilic egg-derived carbon dots: rapid plasma fabrication, pyrolysis process, and multicolor printing patterns. Angew Chem 124:9431–9435

Wang R, Lu KQ, Tang ZR, Xu YJ (2017) Recent progress on carbon quantum dots: synthesis, properties and applications in photocatalysis. J Mater Chem A 5:3717–3734

Wang Y, Zheng J, Wang J, Yang Y, Liu X (2017a) Rapid microwave-assisted synthesis of highly luminescent nitrogen-doped carbon dots for white light-emitting diodes. Opt Mater 73:319–329

Wang Z, Long P, Feng Y, Qin C, Feng W (2017b) Surface passivation of carbon dots with ethylene glycol and their high-sensitivity to Fe^{3+}. RSC Adv 7:2810–2816

Wei J, Liu B, Yin P (2014) Dual functional carbonaceous nanodots exist in a cup of tea. RSC Adv 4:63414–63419

Wen X, Yu P, Toh YR, Ma X, Tang J (2014) On the upconversion fluorescence in carbon nanodots and graphene quantum dots. Chem Commun 50:4703–4706

Wu ZL, Zhang P, Gao MX, Liu CF, Wang W, Leng F, Huang CZ (2013) One-pot hydrothermal synthesis of highly luminescent nitrogen-doped amphoteric carbon dots for bioimaging from Bombyxmori silk–natural proteins. J Mater Chem B 1:2868–2873

Xu X, Ray R, Gu Y, Ploehn HJ, Gearheart L, Raker K, Scrivens WA (2004) Electrophoretic analysis and purification of fluorescent single-walled carbon nanotube fragments. J Am Chem Soc 126:12736–12737

Xu M, Li Z, Zhu X, Hu N, Wei H, Yang Z, Zhang Y (2013) Hydrothermal/solvothermal synthesis of graphene quantum dots and their biological applications. Nano Biomed Eng 5:65–71

Xu Y, Liu J, Gao C, Wang E (2014) Applications of carbon quantum dots in electrochemiluminescence: a mini review. Electrochem Commun 48:151–154

Yan Z, Zhang Z, Chen J (2016) Biomass-based carbon dots: synthesis and application in imatinib determination. Sensors Actuators B Chem 225:469–473

Yang ST, Cao L, Luo PG, Lu F, Wang X, Wang H, Meziani MJ, Liu Y, Qi G, Sun YP (2009) Carbon dots for optical imaging in vivo. J Am Chem Soc 131:11308–11309

Yang P, Zhao J, Wang J, Cui H, Li L, Zhu Z (2015) Pure carbon nanodots for excellent photocatalytic hydrogen generation. RSC Adv 5:21332–21335

Yang X, Yang X, Li Z, Li S, Han Y, Chen Y, Bu X, Su C, Xu H, Jiang Y, Lin Q (2015a) Photoluminescent carbon dots synthesized by microwave treatment for selective image of cancer cells. J Colloid Interface Sci 456:1–6

Yang X, Wang Y, Shen X, Su C, Yang J, Piao M, Jia F, Gao G, Zhang L, Lin Q (2017) One-step synthesis of photoluminescent carbon dots with excitation-independent emission for selective bioimaging and gene delivery. J Colloid Interface Sci 49:1–7

Yu CY, Xuan TT, Chen YW, Zhao ZJ, Sun Z, Li HL (2015) A facile, green synthesis of highly fluorescent carbon nanoparticles from oatmeal for cell imaging. J Mater Chem C 3:9514–9518

Yu H, Shi R, Zhao Y, Waterhouse GI, Wu LZ, Tung CH, Zhang T (2016) Smart utilization of carbon dots in semiconductor photocatalysis. Adv Mater 28:9454–9477

Yuan Y, Guo B, Hao L, Liu N, Lin Y, Guo W, Li X, Gu B (2017) Doxorubicin-loaded environmentally friendly carbon dots as a novel drug delivery system for nucleus targeted cancer therapy. Colloids Surf B Biointerfaces 159:349–359

Zhang J, Yu S (2015) Carbon dots: large-scale synthesis, sensing and bioimaging. Mater Today 19:382–393

Zhang Z, Shan Y, Wang J, Ling H, Zang S, Gao W, Zhao Z, Zhang H (2007) Investigation on the rapid degradation of congo red catalyzed by activated carbon powder under microwave irradiation. J Hazard Mater 147:325–333

Zhang J, Yuan Y, Liang G, Yu SH (2015) Scale-up synthesis of fragrant nitrogen-doped carbon dots from bee pollens for bioimaging and catalysis. Adv Sci 2:1500002

Zhang L, Zheng W, Tang R, Wang N, Zhang W, Jiang X (2016) Gene regulation with carbon-based siRNA conjugates for cancer therapy. Biomaterials 104:269–278

Zhang QQ, Chen BB, Zou HY, Li YF, Huang CZ (2018) Inner filter with carbon quantum dots: a selective sensing platform for detection of hematin in human red cells. Biosens Bioelectron 100:148–154

Zhao QL, Zhang ZL, Huang BH, Peng J, Zhang M, Pang DW (2008) Facile preparation of low cytotoxicity fluorescent carbon nanocrystals by electrooxidation of graphite. Chem Commun 41:5116–5118

Zhao S, Lan M, Zhu X, Xue H, Ng TW, Meng X, Lee CS, Wang P, Zhang W (2015) Green synthesis of bifunctional fluorescent carbon dots from garlic for cellular imaging and free radical scavenging. ACS Appl Mater Interfaces 7:17054–17060

Zhong D, Miao H, Yang K, Yang X (2016) Carbon dots originated from carnation for fluorescent and colorimetric pH sensing. Mater Lett 166:89–92

Zhou J, Booker C, Li R, Zhou X, Sham TK, Sun X, Ding Z (2007) An electrochemical avenue to blue luminescent nanocrystals from multiwalled carbon nanotubes (MWCNTs). J Am Chem Soc 129:744–745

Zhou M, Zhou Z, Gong A, Zhang Y, Li Q (2015) Synthesis of highly photoluminescent carbon dots via citric acid and Tris for iron (III) ions sensors and bioimaging. Talanta 143:107–113

Zhou J, Deng W, Wang Y, Cao X, Chen J, Wang Q, Xu W, Du P, Yu Q, Chen J, Spector M (2016) Cationic carbon quantum dots derived from alginate for gene delivery: one-step synthesis and cellular uptake. Acta Biomater 42:209–219

Zhu CZ, Zhai JF, Dong SJ (2012) Bifunctional fluorescent carbon nanodots: green synthesis via soy milk and application as metal-free electrocatalysts for oxygen reduction. Chem Commun 48:9367–9369

Zhu S, Meng Q, Wang L, Zhang J, Song Y, Jin H, Zhang K, Sun H, Wang H, Yang B (2013) Highly photoluminescent carbon dots for multicolor patterning, sensors, and bioimaging. Angew Chem 125:4045–4049

Zuo J, Jiang T, Zhao X, Xiong X, Xiao S, Zhu Z (2015) Preparation and application of fluorescent carbon dots. J Nanomater 2015:10